Carbohydrate Polymers 83 (2011) 1604–1610

Contents lists available at ScienceDirect

Carbohydrate Polymers

journal homepage: www.elsevier.com/locate/carbpol

# Preparation of starch-based nanoparticles through high-pressure homogenization and miniemulsion cross-linking: Influence of various process parameters on particle size and stability

Ai-min Shi [a], Dong Li [a,*], Li-jun Wang [b], Bing-zheng Li [a], Benu Adhikari [c]

[a] College of Engineering, China Agricultural University, P.O. Box 50, 17 Qinghua Donglu, Beijing 100083, China
[b] College of Food Science and Nutritional Engineering, China Agricultural University, Beijing, China
[c] School of Science and Engineering, University of Ballarat, VIC 3353, Australia

ARTICLE INFO

*Article history:*
Received 31 July 2010
Received in revised form
17 September 2010
Accepted 7 October 2010
Available online 13 October 2010

*Keywords:*
Starch nanoparticles
High-pressure homogenization
Miniemulsion cross-linking

ABSTRACT

A new and convenient synthetic route using high-pressure homogenization combined with water-in-oil (w/o) miniemulsion cross-linking technique was used to prepare sodium trimetaphosphate (STMP)-cross-linked starch nanoparticles. Dynamic light scattering (DLS) and transmission electron microscopy (TEM) revealed that starch nanoparticles had narrow size distribution, good dispersibility and spherical shape. Effect of process parameters (surfactant content, water/oil ratio, starch concentration, homogenization pressure and cycles) on the starch nanoparticle size in miniemulsion was evaluated. We show that there is an optimal surfactant concentration giving rise to smaller starch nanoparticles and better stability. Apart from the water/oil ratio and starch concentration, the homogenization pressure and cycles (passes) also significantly affect the size of starch nanoparticles ($p < 0.05$). The stability analysis of starch nanoparticles in water for 2 h to 2 days and in temperature ranges of 25–45 °C showed firm structure and good stability. These nanoparticles are expected to be exploited as drug carriers.



## 1. Introduction

In recent years nanoparticles (NPs) have drawn considerable attention for their small size, customized surface, improved solubility and multiple functionality (Singh & Lillard, 2009). Many organic and inorganic polymers such as poly(caprolactone) (Calvo, Remuñán-López, Vila-Jato, & Alonso, 1997), poly(ethyleneimine) (Godbey, Wu, & Mikos, 1999), poly (lactic acid) (Zambaux, Bonneaux, Gref, Dellacherie, & Vigneron, 1999), poly(ethylene glycol) (Veiseh, Gunn, & Zhang, 2010), poly(lactic-glycolic acid) (Manchanda, Fernandez-Fernandez, Nagesetti, & McGoron, 2010) and hydroxyapatite (Wu et al., 2010) have been investigated for the preparation of nanoparticles with different characteristics and the development of novel and advanced materials (Ozin & Cademartiri, 2009). Likewise, many researchers have also prepared nanoparticles using natural compounds such as chitosan, dextran, gelatin, alginate, albumin and starch (Aumelas, Serrero, Durand, Dellacherie, & Leonard, 2007; Bertholon, Hommel, Labarre, & Vauthier, 2006; Bravo-Osuna, Schmitz, Bernkop-Schnürch, Vauthier, & Ponchel, 2006; Janes, Fresneau, Marazuela, Fabra, & Alonso, 2001; Liu et al., 2008; Simi & Emilia Abraham, 2007).

Starch is widely used in food, chemical, textile, papermaking, medicine and many other industries because of its biodegradability, reproducibility and cheapness (Hoover, Hughes, Chung, & Liu, 2010; Song et al., 2009). In medical applications, starch is often used as a pharmaceutical excipient and bonding material. However, raw starch has limited applications due to its innate disadvantages such as poor solubility in cold water, tendency to retrograde and high viscosity once it is gelatinized. Therefore, some degree of modification is essential to enhance its functionality. Starch nanoparticle is one of the products of such modification and is used as a vehicle of drug delivery especially in nano-scale drug delivery systems (Santander-Ortega et al., 2010; Simi & Emilia Abraham, 2007).

Starch nanoparticles (StNPs) or nanospheres are nano-sized (1–1000 nm in the pharmaceutical field) particulates of starch prepared by chemically cross-linking starch molecules with appropriate cross-linkers. Once the starch structure is opened and dispersed by the application of alkali, acid and enzymes, the formation of the hydrogen bonds can be accelerated through which such nanoparticles can be formed (Deetae et al., 2008; Hoover, Hughes, Chung, & Liu, 2010). These starch nanoparticles help encapsulate and deliver the hydrophilic drugs to targeted spots, in the absence of which these drugs are sensitive to the environment prevailing in stomach, intestine and blood circulation system. This approach (encapsulation of active drug in starch nanoparticles) minimizes the undesired release of the drug (such as initial burst), improves

* Corresponding author. Tel.: +86 10 62737351; fax: +86 10 62737351.
*E-mail address:* dongli@cau.edu.cn (D. Li).

0144-8617/$ – see front matter © 2010 Elsevier Ltd. All rights reserved.
doi:10.1016/j.carbpol.2010.10.011

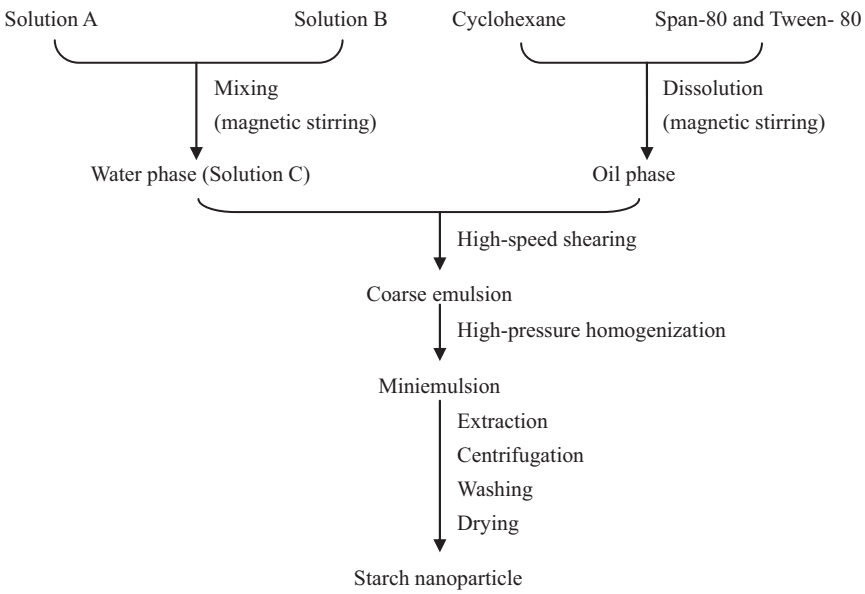


**Fig. 1.** Flow chart of the starch nanoparticle preparation. The composition of solution A and solution B was defined in Table 1; all the process parameters were described in the article.

the efficacy of drug delivery, prolongs the residence time of drugs and reduces the drug-related side effects (Kreuter, 2007; Singh & Lillard, 2009).

Recently, various techniques such as supercritical fluid extraction, solvent evaporation, precipitation and emulsion cross-linking have been used to prepare nanoparticles (Bravo-Osuna, Schmitz, Bernkop-Schnürch, Vauthier, & Ponchel, 2006; Chang, Jian, Yu, & Ma, 2010; Chaudhuri & Paria, 2010; Chavanpatil, Khdair, & Panyam, 2007; Mai Hoa, Chi, Triet, Thanh Nhan, & Chien, 2009; Wang, Smetana, Boeckl, Brown, & Wai, 2009). Among these techniques, supercritical extraction is mainly used to produce inorganic metal nanoparticles. The solvent evaporation requires very large quantity of organic solvent and the precipitation method always involves complicated processing-steps. The emulsion cross-linking techniques, especially the water-in-oil (w/o) emulsion cross-linking has well defined and simple preparation steps with mild processing conditions. Hence this technique could meet the requirement of producing nanoparticles from hydrophilic natural materials such as starch, gelatin and their derivatives (Ethirajan, Schoeller, Musyanovych, Ziener, & Landfester, 2008; Liu et al., 2008).

The (w/o) emulsion cross-linking technique involves the dispersion of the aqueous phase (containing starch and cross-linkers) in the oil phase with the presence of emulsifiers. This emulsion is quite stable and generates starch particles through cross-linking reaction (Ethirajan, Schoeller, Musyanovych, Ziener, & Landfester, 2008). These emulsion droplets help maintain the shape and size of the particles within the dispersed phase. From this technique nanoparticles can easily be obtained if we can produce miniemulsion containing nano-scale droplets. As the miniemulsion is a non-equilibrium system, energy input from chemical potential or mechanical devices is required (Antonietti & Landfester, 2002; Asua, 2002). Miniemulsion can be produced using micro-emulsion method by creating chemical potential through the use of surfactants. However, this method requires large quantity of surfactants compared to the miniemulsion which is obtained using mechanical devices. The former is actually more expensive than the latter method (Antonietti & Landfester, 2002). Although instruments such as rotor–stator emulsifiers, sonicators and high-pressure homogenizers can be used to provide mechanical energy to produce miniemulsions, high-pressure homogenizer is much more efficient than others to prepare nanoparticles (Asua, 2002).

In these contexts, the aim of this study was to investigate a new synthetic route of producing starch nanoparticles using high-pressure homogenizer applied to water-in-oil miniemulsion cross-linking. We assessed various surfactant and starch contents as well as different water/oil ratios. Furthermore, the particle size, stability of the dispersion, rehydration and morphology of the nanoparticles has also been studied.

## 2. Materials and methods

### 2.1. Materials

Water soluble starch was purchased from Beijing Aoboxing Biological Technique Company (Beijing, China). Sodium chloride, sodium hydroxide, cyclohexane, acetone and acetic acid were provided by Beijing Chemical Company (Beijing, China). Tween-80 and Span-80 were purchased from Tianjing Fuchen Chemical Company (Tianjing, China). Sodium trimetaphosphate (STMP) was obtained from Tianjing Dengfeng Chemical Company (Tianjing, China). All of these reagents were of analytical grade and used without further purification. Deionized water was used throughout the work.

### 2.2. Preparation of starch nanoparticles

Starch nanoparticles were created in w/o miniemulsion system using emulsion cross-linking technique with STMP as a cross-linking agent. This method combines the processes used for preparing starch nanoparticles and miniemulsions. The solidification of the starch particles and cross linking reaction takes place during the stable phase of miniemulsion. The flowchart for preparing the starch nanoparticles is provided in Fig. 1. As can be seen from this figure there are five main steps: (1) the water phase was formed by mixing solution A and solution B. Solution A was prepared by dissolving water soluble starch in sodium hydroxide solution and then stirring it for 2 h until the starch was fully dissolved. Solution B was prepared by dissolving STMP in sodium chloride solution. The proportions of starch, sodium hydroxide, sodium chloride and STMP are listed in Table 1. (2) The oil phase was prepared by dissolving the mixture (Table 1) of Span-80 and Tween-80 in cyclohexane and stirring the resultant mixture. The temperature of the oil phase was maintained at 45 °C by a thermostat. (3) The oil phase was stirred

**Table 1**
Composition and ratio of the constituents in water phase and oil phase.

| | Deionised water (g) | Soluble starch (g) | NaOH (g) | STMP[a] (g) | NaCl (g) | Cyclohexane (ml) | Surfactant (g) |
|---|---|---|---|---|---|---|---|
| Solution A | 30 | 8 | 1.5 | 0 | 0 | 0 | 0 |
| Solution B | 20 | 0 | 0 | 2 | 1.5 | 0 | 0 |
| Oil phase | 0 | 0 | 0 | 0 | 0 | 150 | 4.5 (Span-80:Tween-80 = 84:16) |

[a] STMP refers to sodium tripolyphosphate.

at 5000–6000 rpm for 20 s using the high-speed shear apparatus (IKA® T25 digital, Staufen, Germany) and both the solutions A and B were mixed to produce solution C. Then solution C was poured into the oil phase immediately at constant stirring of 10,000 rpm for 2 min (coarse emulsion). (4) The coarse emulsion was subsequently homogenized in a high-pressure homogenizer (ATS® AH-100D, BVI, Canada) at pressures ranging from 10 MPa to 60 MPa for 1–5 passes. (5) The miniemulsion obtained by the following steps 1–4 was kept stirring and the starch in the dispersed phase was cross-linked by the STMP for 3 h (the cross-linking time was calculated from the beginning of the mixing operation to the time when the gel in the bottom cannot fall down after inverting the beaker). The starch nanoparticles were precipitated from the miniemulsion by adding 10% (v/v) acetic and separated from rest of the liquid mixture by centrifugation (3000 rpm). The nanoparticles obtained from the centrifugation process were further purified using acetone and finally washing with water. Subsequently the water was removed by vacuum freeze-drying for 30 h. The dry samples obtained from the vacuum freeze-drying process were packaged in ziplock bags and kept in desiccators for further analysis.

### 2.3. Particle size and distribution analysis

The average size (*Z*-average size) of nanoparticle in miniemulsion as well as in water was measured using a Zetasizer (Nano ZS, Malvern Instruments, Worcestershire, UK). The polydispersity index (PdI) which reflects the range of nanoparticle size can be measured by this instrument, from values lower than 0.1 for suitable measurements and good-quality of the colloidal suspensions to values close to 1 for poor-quality samples which has a very broad size distribution and may contain large particles or aggregates. Specific calculation process is defined in the ISO standard document 13321:1996 E (Malvern Instruments, 2007).

### 2.4. Dispersion and morphology examination

The dispersion of starch nanoparticles in the miniemulsion was observed using a 400× optical microscope coupled with a digital camera (Olympus® CX31, Olympus Instruments, Tokyo, Japan). Although the size of starch nanoparticles in miniemulsion could not be measured within the magnification limit of the microscope, the dispersion situation could be qualitatively illustrated from the images.

The morphological examination of starch nanoparticles after vacuum freeze-drying was performed using a Transmission Electron Microscope (TEM H-800, Hitachi Instruments, Tokyo, Japan). Dried starch nanoparticles were dispersed in alcohol. This suspension was then gently dropped on the copper mesh (3 mm i.d.) and was observed under TEM after drying in air for 10 min.

### 2.5. Statistical analysis

All the experiments were carried out in triplicates and the size data are expressed as mean ± standard deviations. Statistical analysis system (SAS v.9.0, Cary, NC, USA) was used for analysis of variance and significant differences were analyzed by Duncan's multiple range tests at 0.95 confidence level.

## 3. Results and discussion

### 3.1. Preparation of starch nanoparticles

In the dispersed phase of the miniemulsion, the hydroxyl groups of starch molecules reacted with STMP and the starch chains were reorganized into three-dimensional conformation. These macromolecular structures were trapped within nano-scaled droplets and eventually starch nanoparticles were formed. The reaction between STMP and starch can be represented by the chemical formulae below (Fang et al., 2008).

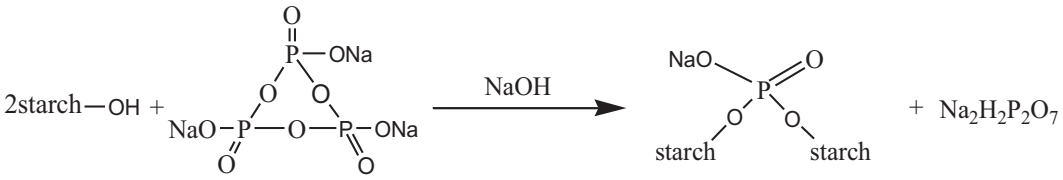


With the composition and ratio of the water and oil phases given in Table 1, we prepared starch nanoparticles using water/oil ratio (v/v) of 15/150 and homogenizing the mixture at 30 MPa and 3 passes. The average size (*Z*-average size) and the spread range of starch nanoparticle were 172.2 ± 1.3 nm and 101.4 ± 7.9 nm, respectively. The size distribution of these particles is presented in Fig. 2(C).

The dispersion of miniemulsion under the 400× optical microscope is provided in Fig. 2(A). This figure shows that there is no aggregation of the dispersed phase droplets which corroborates well with reasonably sharp peak and monodispersion of droplets seen in Fig. 2(C). The dispersed droplets appear to be spherical and intact.

The morphology of the starch nanoparticles is shown in Fig. 2(B), which shows that the most of starch nanoparticles have a good sphericity and the particle size ranges between 50 nm and 250 nm. The TEM image shows that some starch particles are significantly larger and darker than others. This can be attributed to overlapping of nano-particles on the copper mesh during sample preparation, since that as the concentration of starch nanoparticles solution is higher, the quantity of the starch nanoparticles becomes relatively larger, so that the particles will have a trend to aggregate together.

### 3.2. Particle size analysis

The emulsion composition in Tables 2–4 is accordance to the ratio in Table 1. Specifically, the composition of the solution A is 8 g starch, 1.5 g NaOH and 30 g water while the solution B is of 2 g STMP, 1.5 g NaCl and 20 g water. In Table 4, the ratio of the starch,

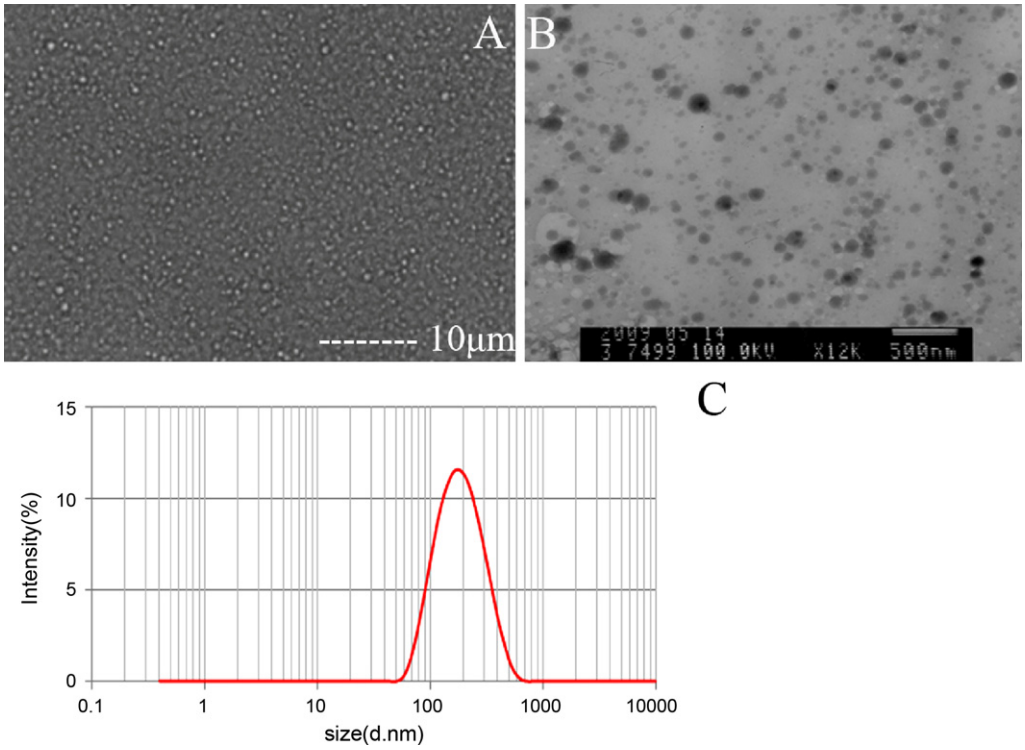


**Fig. 2.** Exterior morphology and particle size distribution of starch nanoparticles. (A) Shows optical microscopic image of miniemulsion (400×); (B) reflects transmission electron micrograph of starch nanoparticles; (C) represents particle size distribution of starch nanoparticles in miniemulsion.

**Table 2**
Effect of the surfactant concentration on the particle size and mean PdI in cyclohexane.

| Concentration (%, w/v) | *Z*-avg (d nm) and mean PdI (in parentheses) | | | | |
|---|---|---|---|---|---|
| | 30 MPa – 1 cycle | 30 MPa – 2 cycles | 30 MPa – 3 cycles | 30 MPa – 4 cycles | 30 MPa – 5 cycles |
| 3 | 273.0 ± 12.8$^{b}$ (0.375) | 266.1 ± 2.3$^{a}$ (0.382) | 180.2 ± 0.9$^{b}$ (0.179) | 167.5 ± 0.7$^{b,a}$ (0.143) | 157.4 ± 0.70$^{b}$ (0.137) |
| 4 | 301.6 ± 2.9$^{a}$ (0.335) | 196.8 ± 2.3$^{b}$ (0.223) | 175.7 ± 1.0$^{c}$ (0.178) | 164.7 ± 1.9$^{b,c}$ (0.165) | 160.4 ± 3.54$^{b}$ (0.155) |
| 5 | 281.5 ± 0.6$^{b}$ (0.309) | 195.6 ± 0.1$^{b}$ (0.218) | 172.6 ± 1.1$^{d}$ (0.168) | 165.1 ± 1.4$^{b,c}$ (0.185) | 159.7 ± 0.14$^{b}$ (0.186) |
| 6 | 223.9 ± 1.8$^{d}$ (0.254) | 185.1 ± 1.0$^{d}$ (0.184) | 166.1 ± 1.3$^{e}$ (0.183) | 158.8 ± 0.6$^{d}$ (0.154) | 152.9 ± 0.78$^{c}$ (0.184) |
| 7 | 245.6 ± 3.2$^{c}$ (0.304) | 189.6 ± 1.4$^{c}$ (0.205) | 173.6 ± 0.8$^{d,c}$ (0.182) | 163.3 ± 0.5$^{c}$ (0.174) | 158.8 ± 0.42$^{b}$ (0.170) |
| 8 | 263.3 ± 12.4$^{c,b}$ (0.327) | 197.3 ± 0.4$^{b}$ (0.210) | 184.1 ± 0.6$^{a}$ (0.208) | 170.5 ± 1.6$^{a}$ (0.177) | 164.2 ± 0.07$^{a}$ (0.178) |

Values of the *Z*-avg represent the mean ± SD ($n = 3$) and values of PdI represent the means of three replicates. Values in a column followed by different lowercase letters in superscripts were significantly different from each other according to Duncan's multiple range tests ($p < 0.05$). Data measured at 25 °C.

NaOH, STMP and NaCl in mixing solution C is 8:1.5:2:1.5 and the usages of water in solution A and solution B are always 30 g and 20 g with the increasing of the other components. For example, when the starch usage is 2 g, there are 0.375 g NaOH, 0.5 g STMP, 0.375 g NaCl and the water in solution A is 30 g, in solution B is 20 g. All these components in the water phase will be cross-linked and turned into starch nanoparticles in the emulsion droplets formed during high-pressure homogenization. The particle size analysis data (*Z*-average size and mean PdI) are presented in Tables 2–5.

### 3.2.1. *Effect of the surfactant content*

As can be seen from Table 2, the size of the starch nanoparticles in cyclohexane is affected by the increase in the surfactant concentration quite significantly in oil phase ($p < 0.05$). Except for the single pass homogenization, the particle size showed a decreasing trend at first and subsequently increased when the concentration of surfactant in the oil phase was increased from 3% to 8% (w/v). The particle size was the lowest (a minimum value) at 6% (w/v) of surfactant concentration. 'The optimal amount' theory provides the

**Table 3**
Effect of the water/oil ratio on the particle size and mean PdI in cyclohexane.

| Ratio (1/150, v/v) | *Z*-avg (d nm) and mean PdI (in parentheses) | | | | |
|---|---|---|---|---|---|
| | 30 MPa – 1 cycle | 30 MPa – 2 cycles | 30 MPa – 3 cycles | 30 MPa – 4 cycles | 30 MPa – 5 cycles |
| 5 | 206.7 ± 1.3$^{f}$ (0.242) | 162.0 ± 1.7$^{f}$ (0.197) | 147.9 ± 0.9$^{e}$ (0.167) | 136.8 ± 0.6$^{f}$ (0.168) | 132.2 ± 1.6$^{e}$ (0.171) |
| 10 | 223.3 ± 0.1$^{e}$ (0.266) | 181.1 ± 0.6$^{e}$ (0.202) | 164.0 ± 0.2$^{d}$ (0.162) | 156.2 ± 0.1$^{e}$ (0.147) | 149.6 ± 0.6$^{d}$ (0.166) |
| 15 | 262.6 ± 3.2$^{d}$ (0.351) | 191.1 ± 1.5$^{d}$ (0.221) | 175.6 ± 0.4$^{d,c}$ (0.170) | 165.0 ± 1.7$^{d}$ (0.181) | 160.3 ± 1.5$^{c}$ (0.200) |
| 20 | 246.5 ± 0.4$^{c}$ (0.301) | 195.5 ± 1.3$^{c}$ (0.225) | 180.7 ± 0.1$^{c}$ (0.201) | 173.2 ± 0.3$^{c}$ (0.190) | 164.8 ± 0.1$^{c}$ (0.172) |
| 25 | 292.9 ± 6.3$^{b}$ (0.388) | 229.6 ± 2.1$^{b}$ (0.246) | 199.9 ± 0.6$^{b}$ (0.225) | 188.9 ± 2.8$^{b}$ (0.221) | 182.7 ± 1.7$^{b}$ (0.213) |
| 30 | 316.2 ± 5.4$^{a}$ (0.336) | 292.8 ± 0.1$^{a}$ (0.451) | 281.7 ± 13.7$^{a}$ (0.435) | 245.0 ± 6.5$^{a}$ (0.371) | 221.3 ± 4.2$^{a}$ (0.307) |

Values of the Z-avg represent the means ± SD ($n = 3$) and values of PdI represent the mean of three replicates. Values in a column followed by different lowercase letters in superscript were significantly different from each as determined by Duncan's multiple range tests ($p < 0.05$). Data measured at 25 °C.

**Table 4**
Effect of the composition of water phase on the particle size and mean PdI in cyclohexane.

| Content (1/50, w/w) | *Z*-avg (d nm) and mean PdI (in parentheses) | | | | |
|---|---|---|---|---|---|
| | 30 MPa – 1 cycle | 30 MPa – 2 cycles | 30 MPa – 3 cycles | 30 MPa – 4 cycles | 30 MPa – 5 cycles |
| 2 | 169.4 ± 1.3$^{c}$ (0.128) | 145.0 ± 0.1$^{d}$ (0.095) | 134.1 ± 0.2$^{d}$ (0.102) | 124.0 ± 0.6$^{d}$ (0.115) | 119.9 ± 0.4$^{d}$ (0.101) |
| 4 | 182.1 ± 0.8$^{c}$ (0.160) | 154.1 ± 0.2$^{d}$ (0.131) | 139.2 ± 1.1$^{d}$ (0.127) | 130.8 ± 0.7$^{d}$ (0.121) | 125.1 ± 1.1$^{d}$ (0.128) |
| 6 | 208.7 ± 1.4$^{c}$ (0.233) | 177.3 ± 7.2$^{c}$ (0.191) | 164.7 ± 7.7$^{c}$ (0.191) | 152.0 ± 0.4$^{c}$ (0.212) | 145.2 ± 1.3$^{c}$ (0.144) |
| 8 | 223.9 ± 1.8$^{c}$ (0.254) | 185.1 ± 1.0$^{c}$ (0.184) | 166.1 ± 1.2$^{c}$ (0.184) | 158.8 ± 0.6$^{c}$ (0.154) | 152.9 ± 0.8$^{c}$ (0.184) |
| 10 | 444.8 ± 9.3$^{b}$ (0.561) | 289.5 ± 2.3$^{b}$ (0.409) | 327.4 ± 12.7$^{b}$ (0.450) | 254.7 ± 5.5$^{b}$ (0.378) | 281.9 ± 5.2$^{b}$ (0.433) |
| 12 | 802.5 ± 77.1$^{a}$ (1) | 463.6 ± 17.0$^{a}$ (0.732) | 408.1 ± 18.7$^{a}$ (0.670) | 387.4.0 ± 4.8$^{a}$ (0.512) | 416.3 ± 15.8$^{a}$ (0.626) |

Values of the *Z*-avg represent the means ± SD ($n = 3$) and values of PdI represent the means of three replicates. Values in a column followed by different lowercase letters as superscripts were significantly different from each other according to Duncan's multiple range tests ($p < 0.05$). Data measured at 25 °C.

possible explanation for this phenomenon. According to this theory certain quantity of surfactant optimally covers the surface area of the droplets which provides maximum stability against (emulsion) droplet coalescence. This can be manifested into smallest emulsion (droplet) sizes. When the amount of surfactant is not enough to completely coat the entire surface area of the droplets after homogenization process, the droplets tend to aggregate with each other to reduce the surface area (Niemann & Sundmacher, 2010). Instead, if there is an excess surfactant in the oil phase, free emulsifier molecules will be formed within the emulsion which will ultimately adhere to the droplets and will be covered by excess amount of surfactant. Both of the above scenarios can absorb and disperse the energy of emulsification. As a consequence, the energy available for repelling or pushing the droplets apart decreases which results in the increase in the droplets size. These results show that the getting the surfactant content right or determining the optimal amount of surfactant for optimally coating the surface of the final droplets is a critical step. Asua (2002) reported that the smallest size emulsion droplets can be obtained using high-pressure homogenization technology compared to other existing methods, such as ultrasonic emulsification and high shear emulsification. These results also show that the nanoparticles in the droplets would be the smallest when optimal surfactant concentration is used while preparing the miniemulsion. Similar observations regarding the effect of surfactant concentration on the nanoparticles were made by Antonietti and Landfester (2002) and Asua (2002).

### 3.2.2. *Effect of the water/oil ratio*

The effect of the water/oil ratio (in miniemulsion) on the particle size of the starch nanoparticles in cyclohexane is given in Table 3. This table reveals that the increase in the water/oil ratio increases the particle size significantly ($p < 0.05$). The particle size increased from 206.7 nm to 316.2 nm (1 pass through the homogenizer), 162.0 nm to 292.8 nm (2 passes), 147.9 nm to 281.7 nm (3 passes), 136.8 nm to 245.0 nm (4 passes), and 132.2 nm to 221.3 nm (5 passes) when the water/oil ratio increased from 5/150 (v/v) to 30/150 (v/v). One of the possible reasons for this increase may be due to the fact that when the volume of the water phase is increased, higher power input would be required during the emulsification process to reduce the droplet size. Under the same energy level (same homogenization cycles) the size of the droplets would become larger when the water/oil ratio is increased. This will eventually lead to the increase in the size of the starch nanoparticles in the emulsion droplets. Furthermore, at larger water/oil ratios of coarse emulsion, the possibility of incomplete homogenization of the coarse emulsion increases when higher water/oil ratios are used. In this situation relatively larger starch nanoparticles will be produced compared to the ones formed from lower water/oil ratios (Antonietti & Landfester, 2002). The other possible reason is that when increasing the water/oil ratio, there would be relatively less emulsifier, which caused a lower surface tension of the droplets, resulting in a bigger particle size. Such an effect of the water/oil ratio is similar to the effect of the surfactant content.

### 3.2.3. *Effect of the starch concentration*

We varied the soluble starch content in solution A from 2 g to 12 g and also reduced the amount of other components (except water) according to the proportion in Table 1. The *Z*-average sizes of the starch nanoparticles thus obtained are presented in Table 4. This table shows remarkable increase in particle size when the starch-STMP content was increased in water phase. The increase in particle size to this extent could be explained by the increase in the cross-linking reaction intensity. Our preliminary work indicated that the cross-linking reaction was closely associated with the concentration of reactants. For example, 8.0 g soluble starch, 1.5 g NaOH, 2.0 g STMP and 1.5 g NaCl in 50.0 g DI water could be cross-linked completely within 20 min. The reaction time was reduced to 5 min if the reactant composition was maintained at 12.0 g soluble starch, 2.25 g NaOH, 3 g STMP and 2.25 g NaCl. Quite contrary to this, the reaction time was prolonged to 1 h when the concentration of the reactants in the system was decreased to maintain at 2.0 g soluble starch, 0.375 g NaOH, 0.5 g STMP and 0.375 g NaCl. It has to be mentioned here that the reaction time reflects the intensity of cross-linking and the apparent kinetics of cross-linking reaction differs with the intensity of cross-linking. Because of this reason the reaction time affects the viscosity of both the water phase and the emulsion. The variation in the solution viscosity means that the emulsion process requires different level of energy input to

**Table 5**
Effect of the homogenization process on the particle size and PdI in cyclohexane.

| Pressure (MPa) | *Z*-avg (d nm) and mean PdI (in parentheses) | | | | |
|---|---|---|---|---|---|
| | 1 Cycle | 2 Cycles | 3 Cycles | 4 Cycles | 5 Cycles |
| 10 | 354.6 ± 40.9$^{a}$ (0.445) | 278.0 ± 28.6$^{a}$ (0.429) | 260.4 ± 10.9$^{a}$ (0.134) | 250.1 ± 6.5$^{a}$ (0.203) | 236.4 ± 7.3$^{a}$ (0.023) |
| 20 | 235.9 ± 35.6$^{b}$ (0.273) | 190.5 ± 14.0$^{b}$ (0.197) | 186.1 ± 0.1$^{b}$ (0.175) | 176.7 ± 1.7$^{b}$ (0.123) | 176.1 ± 3.5$^{b}$ (0.166) |
| 30 | 223.3 ± 0.1$^{b,c}$ (0.266) | 181.1 ± 0.6$^{c,b}$ (0.202) | 164.0 ± 0.2$^{c}$ (0.162) | 156.2 ± 0.1$^{c}$ (0.147) | 149.6 ± 0.6$^{c}$ (0.167) |
| 40 | 207.8 ± 5.9$^{b,c}$ (0.185) | 174.0 ± 1.7$^{c,b,d}$ (0.157) | 160.5 ± 1.5$^{c,d}$ (0.152) | 151.8 ± 1.9$^{c}$ (0.149) | 145.4 ± 0.4$^{c}$ (0.151) |
| 50 | 190.4 ± 3.3$^{b,c}$ (0.184) | 160.7 ± 1.8$^{c,d}$ (0.153) | 153.6 ± 0.8$^{d}$ (0.101) | 140.6 ± 0.6$^{d}$ (0.141) | 135.9.1 ± 0.5$^{d}$ (0.124) |
| 60 | 184.0 ± 0.2$^{c}$ (0.153) | 152.7 ± 1.0$^{d}$ (0.156) | 138.1 ± 1.6$^{e}$ (0.148) | 128.9 ± 1.3$^{e}$ (0.149) | 123.3 ± 1.0$^{e}$ (0.162) |

Values of the *Z*-avg represent the means ± SD ($n = 3$) and values of PdI represent the means of three replicates. Values in a column followed by different lowercase letters as superscripts were significantly different from each other according to Duncan's multiple range tests ($p < 0.05$). Data measured at 25 °C.

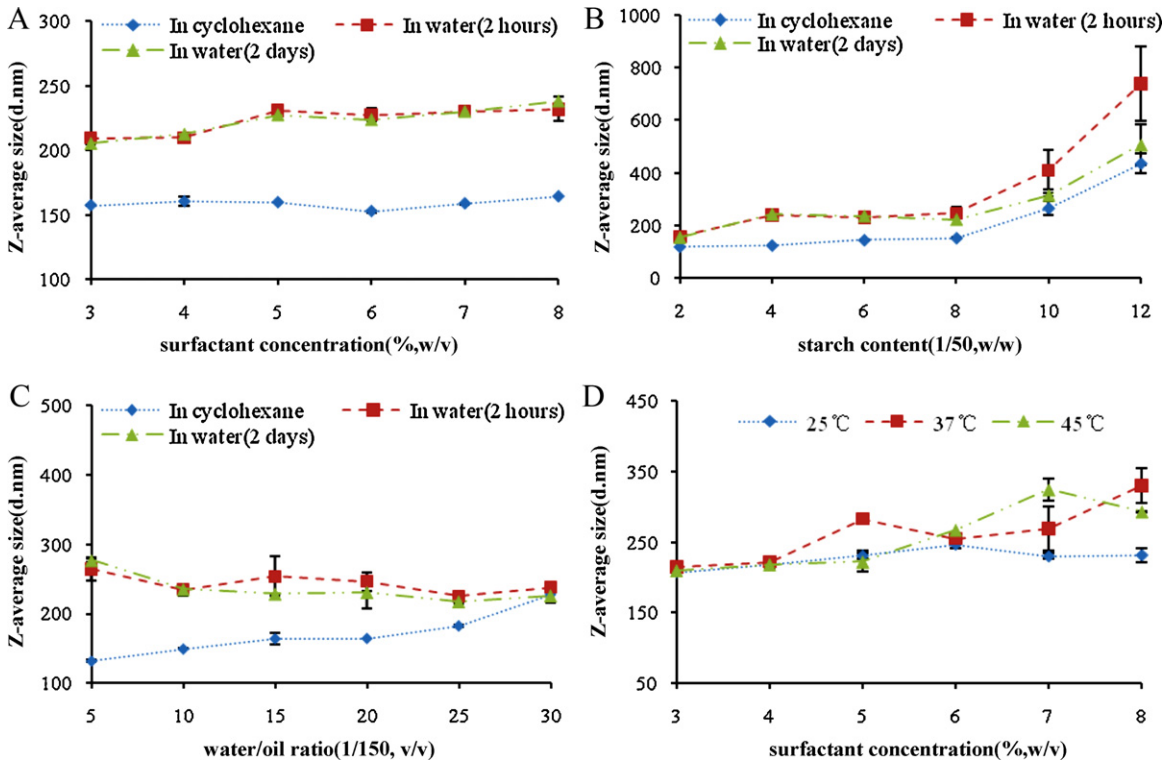


**Fig. 3.** Particle stability analysis of starch nanoparticles. (A–C) Represent effect of the dispersion medium on particle size; (D) reflects effect of temperature on the on particle size.

create the miniemulsions which eventually results in variation in the size of starch nanoparticles (the reaction time, also called as cross-linking time, was calculated from the beginning of the mixing operation to the time when the gel in the bottom cannot fall down after inverting the beaker).

### 3.2.4. Effect of the homogenization pressure

The effect of homogenization pressure on the particle size was investigated by varying the homogenization pressure from 10 MPa to 60 MPa and the results are presented in Table 5. As can be seen from this table, the particle size decreased when the pressure increased from 10 MPa to 20 MPa. However, the extent of variation is quite small when pressure varies from 20 MPa to 60 MPa. One of the explanation for this two tiered particle reduction is that although the energy supplied by the homogenization process was sufficient to reduce size of droplets from micron to nano size, this energy level may be insufficient to further break the droplets into further smaller in size of nano scale. At the homogenization pressure of 10 MPa, the energy supplied is mainly utilized in forming nano-sized droplets of the w/o coarse emulsion; while the energy supplied at higher homogenization pressures (20–60 MPa) is clearly utilized to reduce the size of the nano-sized droplets further (Asua, 2002). In other words, greater the homogenization pressure above the threshold value of 10 MPa (i.e. 20–60 MPa or greater), the size of the emulsion droplets as well as the starch nanoparticles inside these emulsion droplets can become much smaller.

### 3.2.5. Effect of the homogenization cycles (passes)

The influence of the homogenization cycles (passes) on the size of the starch nanoparticles can be observed from Table 2 to Table 5. Similar to the effect of the homogenization pressure on particle size, a two-cycle (pass) homogenization could decrease the particle size significantly compared to the corresponding particle size from the one-pass homogenization. However, when the homogenization passes of more than two (e.g. 3–5 passes) were used the extent of reduction in particle size became relatively smaller. This could be attributed to the efficiency of homogenization. The energy supplied by single homogenization pass could be mainly utilized to reduce the particle size from micron to nano scale; while energy supplied by higher homogenization cycles (e.g. 2–5 homogenization passes) can be insufficient to generate the change in the particle size to the same extent.

## 3.3. Particle stability analysis

As can be seen from Fig. 3(A–D), there are two different emulsions i.e. w/o emulsion and water solution. In the w/o emulsion, the composition of the elements is according to the ratio in Table 1. The starch nanoparticles are solidified through the cross-linking process into spherical colloidal particles. The whole emulsion is full of these particles which are covered by the emulsifiers while the main part is still oil phase such as cyclohexane. In water solution, all the starch nanoparticles are swelling without dissolving into water and the network structure formed by the cross-linking process was firm enough to resistant the effect of the water. This also can be seen from the small variation of the particle size in water for several hours in Fig. 3(A–D).

### 3.3.1. Effect of dispersion medium

The effect of dispersion medium on the size of the starch nanoparticles and their stability in water could be observed in Fig. 3(A–C). These nanoparticles were prepared using 30 MPa and 5 cycles. These figures show that different dispersion medium can result in significant changes in the particle size of starch nanoparticles. One of the reasons for this variation could be that in the cyclohexane starch nanoparticles are trapped in droplets covered with surfactant which is accessible only to a small amount of water. While in water medium starch nanoparticles could absorb water and undergo greater extent of swelling. However, in longer times

in aqueous medium (for 2 h to 2 days) the size of starch nanoparticles did not change further. Thus, starch nanoparticles could have a stable structure when they are dispersed in water medium for longer times.

### 3.3.2. Effect of temperature

The effect of temperature on the stability of starch nanoparticles in water medium is shown in Fig. 3(D). These starch nanoparticles were produced using 30 MPa and 5 homogenization cycles with various surfactant concentrations. As can be seen from this figure, when the temperature was increased from 25 °C to 45 °C, the change in the particle size was about 100 nm. This increase in particle size due to rise in temperature can be attributed to the network in starch nanoparticles. The network formed by chemical bonding such as hydrogen bonds and covalent bonds might have altered when the temperature of medium was increased resulting in increase in the particle size. However, the effect of temperature rise (from 25 °C to 45 °C) was not strong enough to break such chemical bonding, and that the starch nanoparticles were stable enough to resist the further increase in their size.

## 4. Conclusions

Sodium trimetaphosphate (STMP)-cross-linked starch nanoparticles were successfully produced using high-pressure homogenization technique combined with miniemulsion cross-linking. Starch nanoparticles so produced displayed good sphericity in shape and a comparatively uniform size distribution.

This study also demonstrated that when judicious amount of surfactant in oil is used, sufficiently small size particles with good stability could be produced. The water/oil ratio, concentration of cross-linking reactants in aqueous phase, homogenization pressure and number of homogenization cycles (passes) could significantly affect the size of starch nanoparticles. With judicious manipulations of these parameters, starch nanoparticles with desired particle size and size distribution could be produced. These starch nanoparticles could be swelled in water and they can be stable in water for several days. We also found that these nanoparticles were not affected by temperature of dispersion medium within 25–45 °C. This makes them suitable as drug carriers for *in vivo* delivery as they are very stable at body temperature.

## Acknowledgments

Supported by Program for New Century Excellent Talents in University of China (NCET-08-0537), National Natural Science Foundation of China (30800662), Science and Technology Support Project of China (2009BADA0B03), and High Technology Research and Development Program of China (2009AA043601).

## References

Antonietti, M., & Landfester, K. (2002). Polyreactions in miniemulsions. *Progress in Polymer Science*, *27*, 689–757.

Asua, J. M. (2002). Miniemulsion polymerization. *Progress in Polymer Science*, *27*, 1283–1346.

Aumelas, A., Serrero, A., Durand, A., Dellacherie, E., & Leonard, M. (2007). Nanoparticles of hydrophobically modified dextrans as potential drug carrier systems. *Colloids and Surfaces B: Biointerfaces*, *59*, 74–80.

Bertholon, I., Hommel, H., Labarre, D., & Vauthier, C. (2006). Properties of polysaccharides grafted on nanoparticles investigated by EPR. *Langmuir*, *22*, 5485–5490.

Bravo-Osuna, I., Schmitz, T., Bernkop-Schnürch, A., Vauthier, C., & Ponchel, G. (2006). Elaboration and characterization of thiolated chitosan-coated acrylic nanoparticles. *International Journal of Pharmaceutics*, *316*, 170–175.

Calvo, P., Remuñán-López, C., Vila-Jato, J. L., & Alonso, M. J. (1997). Development of positively charged colloidal drug carriers: Chitosan-coated polyester nanocapsules and submicron-emulsions. *Colloid Polymer Science*, *275*, 46–53.

Chang, P. R., Jian, R., Yu, J., & Ma, X. (2010). Fabrication and characterisation of chitosan nanoparticles/plasticised-starch composites. *Food Chemistry*, *120*, 736–740.

Chaudhuri, R. G., & Paria, S. (2010). Synthesis of sulfur nanoparticles in aqueous surfactant solutions. *Journal of Colloid and Interface Science*, *343*, 439–446.

Chavanpatil, M. D., Khdair, A., & Panyam, J. (2007). Surfactant-polymer nanoparticles: A novel platform for sustained and enhanced cellular delivery of water-soluble molecules. *Pharmaceutical Research*, *24*, 803–810.

Deetae, P., Shobsngob, S., Varanyanond, W., Chinachoti, P., Naivikul, O., & Varavinit, S. (2008). Preparation, pasting properties and freeze–thaw stability of dual modified crosslink-phosphorylated rice starch. *Carbohydrate Polymers*, *73*, 351–358.

Ethirajan, A., Schoeller, K., Musyanovych, A., Ziener, U., & Landfester, K. (2008). Synthesis and optimization of gelatin nanoparticles using the miniemulsion process. *Biomacromolecules*, *9*, 2383–2389.

Fang, Y.-Y., Wang, L.-J., Li, D., Li, B.-Z., Bhandari, B., Chen, X.-D., et al. (2008). Preparation of crosslinked starch microspheres and their drug loading and releasing properties. *Carbohydrate Polymers*, *74*, 379–384.

Godbey, W. T., Wu, K. K., & Mikos, A. G. (1999). Tracking the intracellular path of poly(ethylenimine)/DNA complexes for gene delivery. *Proceedings of the National Academy of Sciences of the United States of America*, *96*, 5177–5181.

Hoover, R., Hughes, T., Chung, H. J., & Liu, Q. (2010). Composition, molecular structure, properties, and modification of pulse starches: A review. *Food Research International*, *43*, 399–413.

Janes, K. A., Fresneau, M. P., Marazuela, A., Fabra, A., & Alonso, M. J. (2001). Chitosan nanoparticles as delivery systems for doxorubicin. *Journal of Controlled Release*, *73*, 255–267.

Kreuter, J. (2007). Nanoparticles—A historical perspective. *International Journal of Pharmaceutics*, *331*, 1–10.

Liu, J., Wang, F.-H., Wang, L.-L., Xiao, S.-Y., Tong, C.-Y., Tang, D.-Y., et al. (2008). Preparation of fluorescence starch-nanoparticle and its application as plant transgenic vehicle. *Journal of Central South University of Technology (English Edition)*, *15*, 768–773.

Mai Hoa, L. T., Chi, N. T., Triet, N. M., Thanh Nhan, L. N., & Chien, D. M. (2009). Preparation of drug nanoparticles by emulsion evaporation method. *Journal of Physics: Conference Series*, doi: 10.1088/1742-6596/187/1/012047.

Malvern Instruments (2007). Zetasizer nano user manual. Malvern Instruments Ltd., Worcestershire WR14 1XZ, UK.

Manchanda, R., Fernandez-Fernandez, A., Nagesetti, A., & McGoron, A. J. (2010). Preparation and characterization of a polymeric (PLGA) nanoparticulate drug delivery system with simultaneous incorporation of chemotherapeutic and thermo-optical agents. *Colloids and Surfaces B: Biointerfaces*, *75*, 260–267.

Niemann, B., & Sundmacher, K. (2010). Nanoparticle precipitation in microemulsions: Population balance model and identification of bivariate droplet exchange kernel. *Journal of Colloid and Interface Science*, *342*, 361–371.

Ozin, G. A., & Cademartiri, L. (2009). Nanochemistry: What is next? *Small*, *5*, 1240–1244.

Santander-Ortega, M. J., Stauner, T., Loretz, B., Ortega-Vinuesa, J. L., Bastos-González, D., Wenz, G., et al. (2010). Nanoparticles made from novel starch derivatives for transdermal drug delivery. *Journal of Controlled Release*, *141*, 85–92.

Simi, C. K., & Emilia Abraham, T. (2007). Hydrophobic grafted and cross-linked starch nanoparticles for drug delivery. *Bioprocess and Biosystems Engineering*, *30*, 173–180.

Singh, R., & Lillard, J. W., Jr. (2009). Nanoparticle-based targeted drug delivery. *Experimental and Molecular Pathology*, *86*, 215–223.

Song, H., Wu, D., Zhang, R.-Q., Qiao, L.-Y., Zhang, S.-H., Lin, S., et al. (2009). Synthesis and application of amphoteric starch graft polymer. *Carbohydrate Polymers*, *78*, 253–257.

Wang, J. S., Smetana, A. B., Boeckl, J. J., Brown, G. J., & Wai, C. M. (2009). Depositing ordered arrays of metal sulfide nanoparticles in nanostructures using supercritical fluid carbon dioxide. *Langmuir*, *26*, 1117–1123.

Wu, Y., Jiang, W., Wen, X., He, B., Zeng, X., Wang, G., et al. (2010). A novel calcium phosphate ceramic–magnetic nanoparticle composite as a potential bone substitute. *Biomedical Materials*, doi: 10.1088/1748-6041/5/1/015001.

Veiseh, O., Gunn, J. W., & Zhang, M. (2010). Design and fabrication of magnetic nanoparticles for targeted drug delivery and imaging. *Advanced Drug Delivery Reviews*, *62*, 284–304.

Zambaux, M. F., Bonneaux, F., Gref, R., Dellacherie, E., & Vigneron, C. (1999). Preparation and characterization of protein C-loaded PLA nanoparticles. *Journal of Controlled Release*, *60*, 179–188.